Supporting Information

Enhancing electrocatalytic CO_2 reduction via engineering substrate-cluster interaction

Qian Sun [a], Huiru Yang [a,*], Chunmei Zhang [a, c*], Aijun Du [b]

[a] *School of Physics, Northwest University, Xi'an 710127, China*
[b] *School of Chemistry and Physics and QUT Center for Materials Science, Queensland University of Technology (QUT), Brisbane, QLD 4000, Australia*
[c] *Shaanxi Key Laboratory for Theoretical Physics Frontiers, Xi'an 710127, China*
Email: y1573349346@163.com;
chunmeizhang@nwu.edu.cn

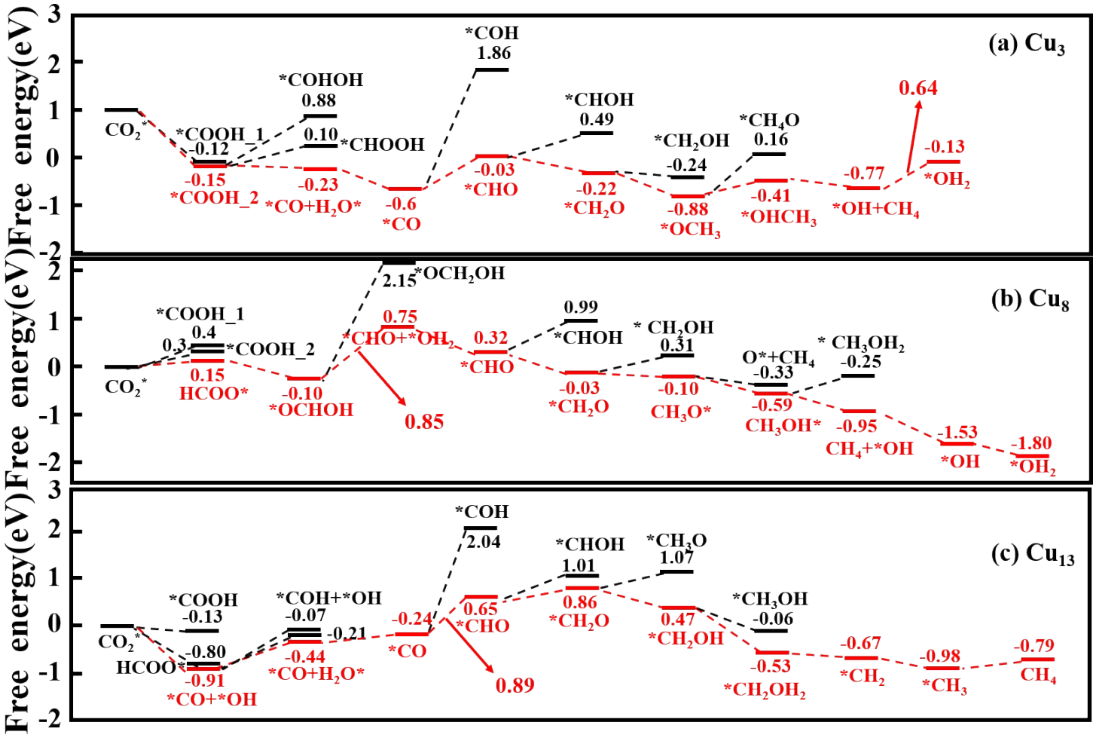

Fig. S1. Free energy diagram and the corresponding geometries of reaction intermediates/products along the most favorable pathway for the CO_2RR of CO_2 molecule on (a) Cu_3, (b) Cu_8, and (c) Cu_{13}.

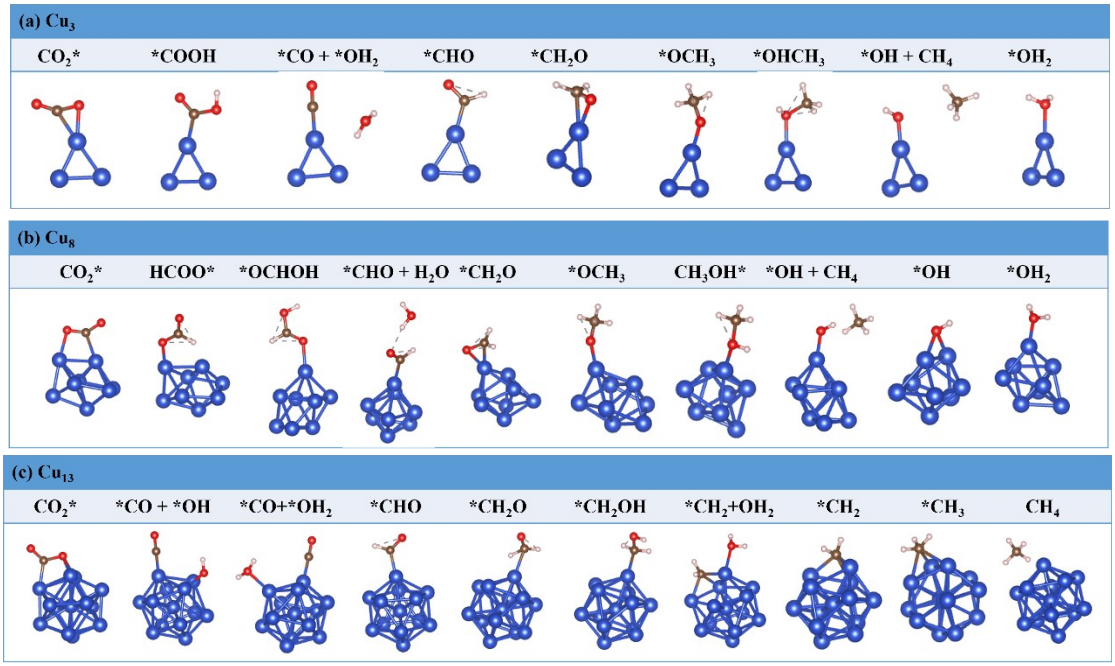

Fig. S2. The optimized CO_2RR intermediates along the most favorable pathway on (a) Cu_3, (b) Cu_8, and (c) Cu_{13}.

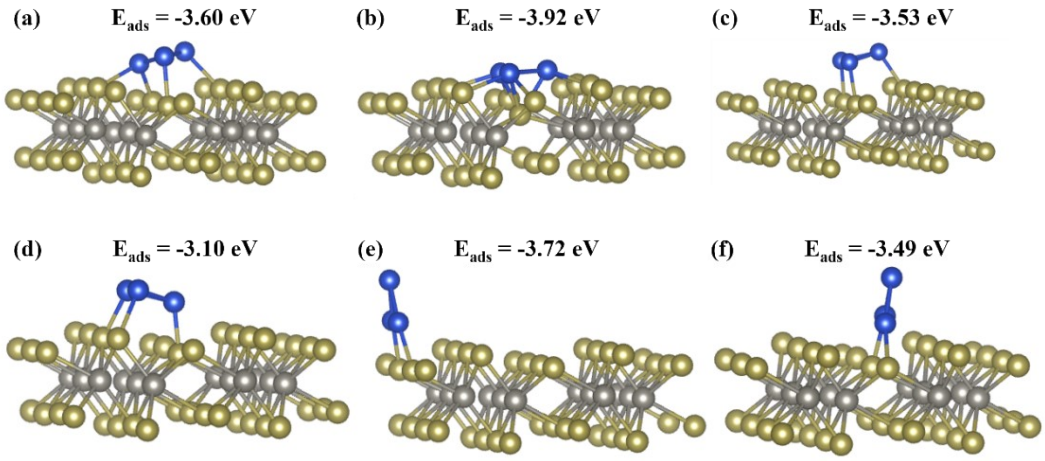

Fig. S3. The optimized configurations and corresponding adsorption energies for Cu_3 clusters anchoring on the T'-WTe_2 surface. Cu, W, and Te atoms are denoted by blue, grey, and orange spheres, respectively. The most stable configuration is shown in Fig. b.

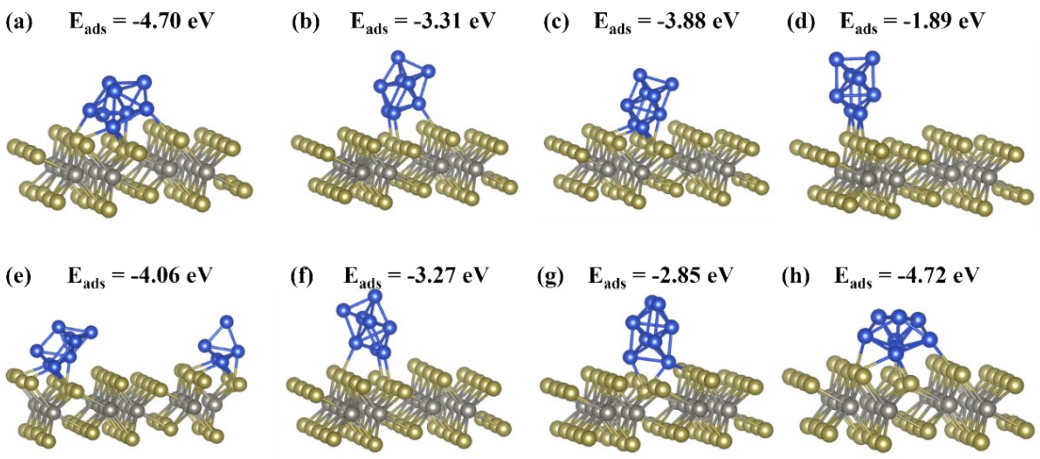

Fig. S4. The optimized configurations and corresponding adsorption energies for Cu_8 clusters anchoring on the T'-WTe_2 surface. Cu, W, and Te atoms are denoted by blue, grey, and orange spheres, respectively. The most stable configuration is shown in Fig. h.

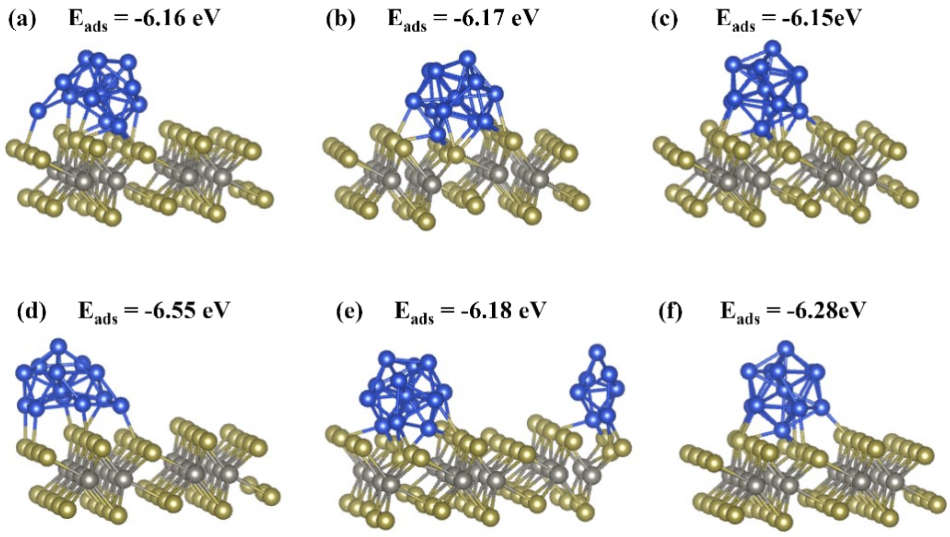

Fig. S5. The optimized configurations and corresponding adsorption energies for Cu_{13} clusters anchoring on the T'-WTe_2 surface. Cu, W, and Te atoms are denoted by blue, grey, and orange spheres, respectively. The most stable configuration is shown in Fig. d.

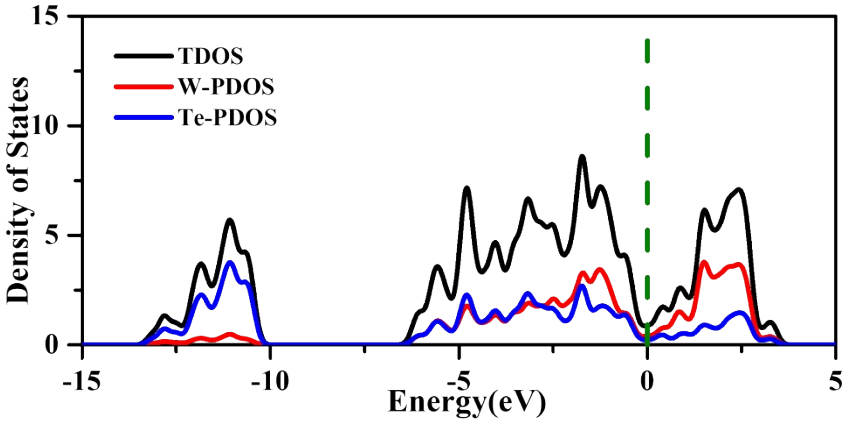

Fig. S6 Total density of states (TDOS) and PDOS of T'-WTe_2.

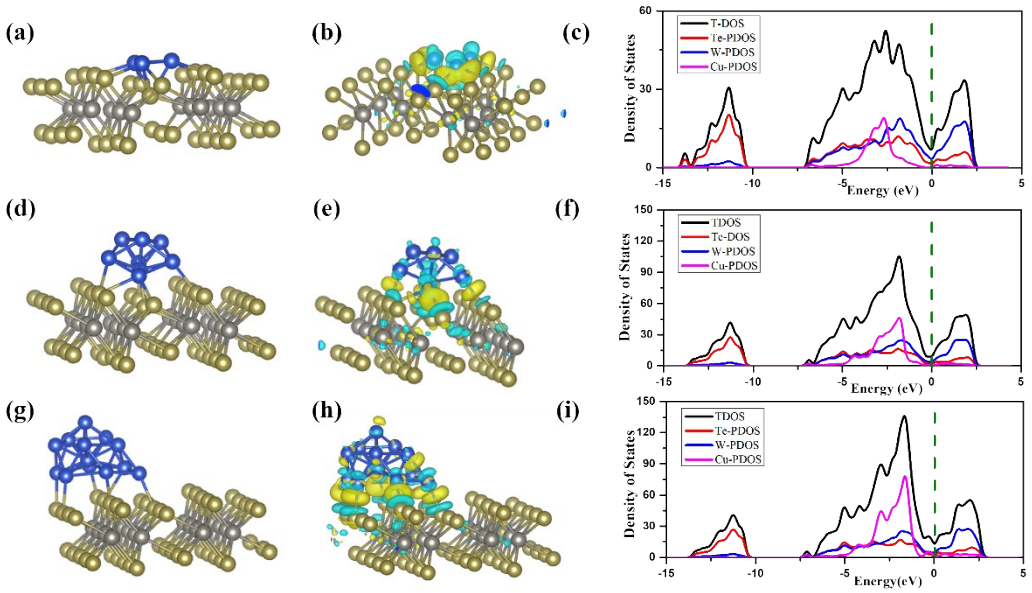

Fig. S7. The most stable configuration for (a) Cu_3@WTe_2 , (d) Cu_8@WTe_2, and (g) Cu_{13}@WTe_2; and the isosurface of the charge density difference for (b) Cu_3@WTe_2, (e) Cu_8@WTe_2, and (h) Cu_{13}@WTe_2; Cu, W, and Te atoms are denoted by grey, light blue, and orange spheres, respectively. The blue (yellow) wireframes denote the loss (gain) of electrons with the isosurface values set as 0.003 $Å^{-3}$; TDOS and PDOS for the W, Te and Cu atoms of (c) Cu_3@WTe_2, (f) Cu_8@WTe_2, and (i) Cu_{13}@WTe_2. The Fermi level is assigned at 0 eV.

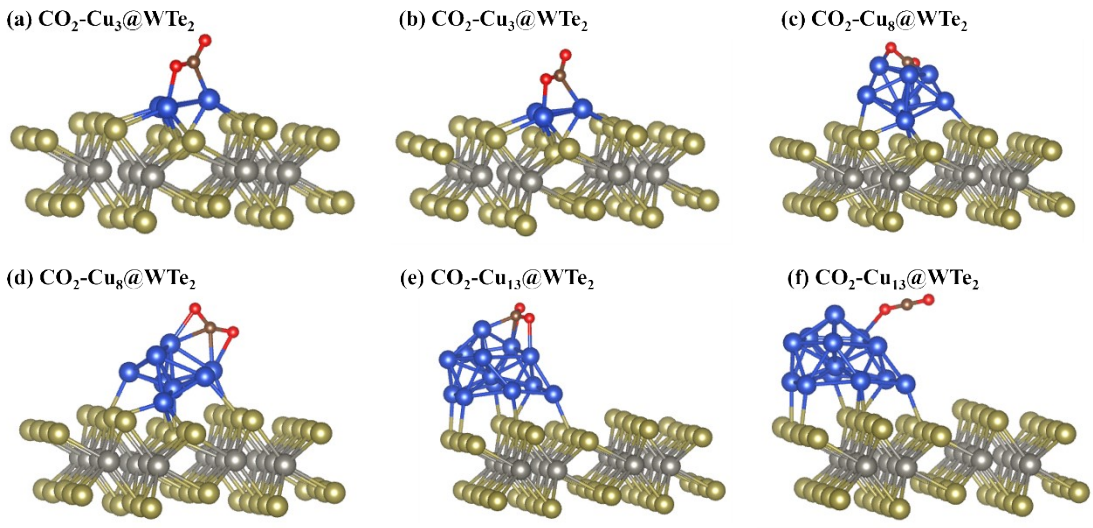

Fig. S8. The optimized configurations for CO_2 adsorption on Cu_n@T'-WTe_2. Cu, W, Te, C and O atoms are denoted by blue, grey, orange, light orange and red spheres, respectively. The most stable configuration for Cu_3@WTe_2 (a), Cu_8@WTe_2 (c) and Cu_{13}@WTe_2 (e).

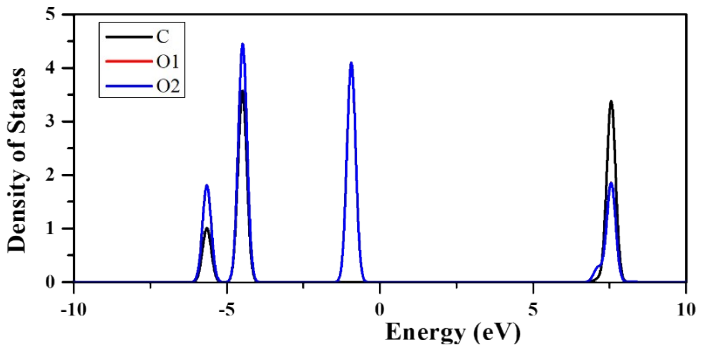

Figure S9. PDOS plots for the C and O atoms in isolated CO_2 molecules.

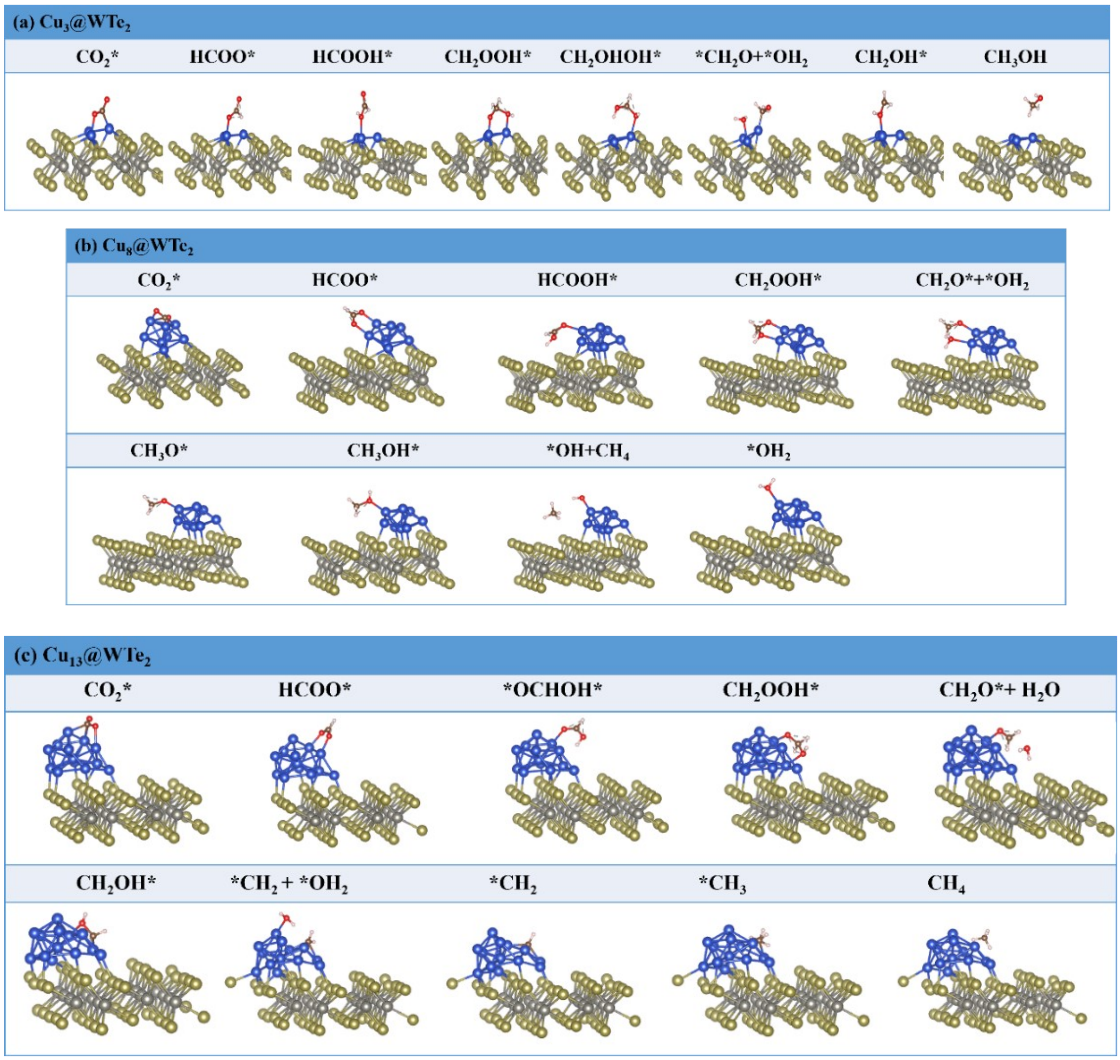

Fig. S10. The optimized CO_2RR intermediates along the most favorable pathway on (a) Cu_3@WTe_2, (b) Cu_8@WTe_2, and (c) Cu_{13}@WTe_2.

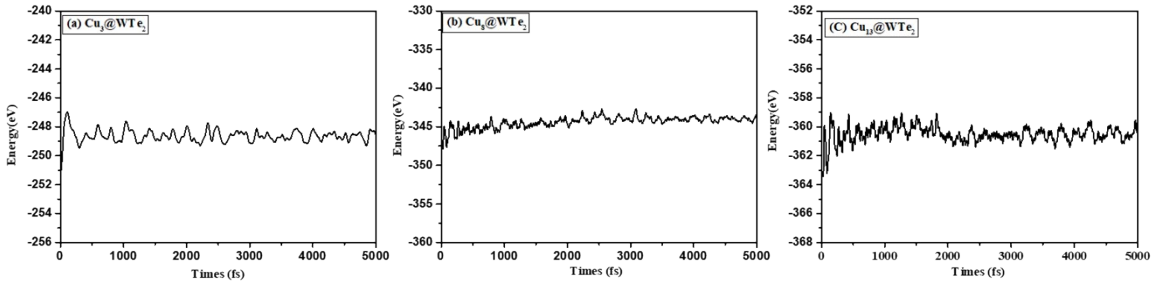

Fig. S11. Total energy of (a) Cu_3@WTe_2, (b) Cu_8@WTe_2, and (c) Cu_{13}@WTe_2 as a function of time step in AIMD simulations at 500 K.

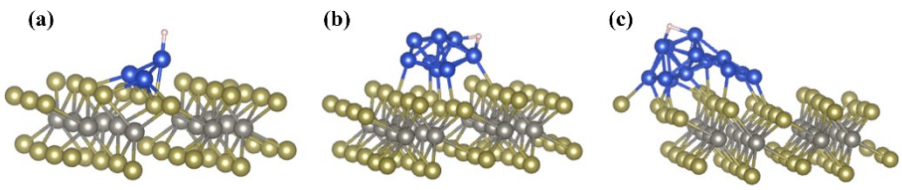

Fig. S12. The optimized configurations for H adsorption on (a) Cu_3@WTe_2, (b) Cu_8@WTe_2, and (c) Cu_{13}@WTe_2.

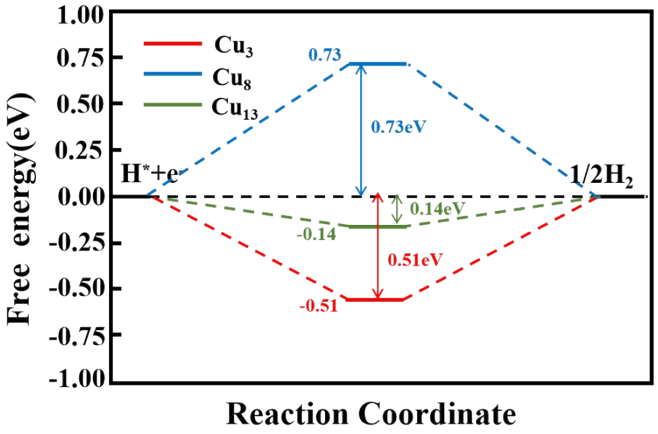

Fig. S13. The free energy changes for hydrogen evolution reaction (HER) on Cu_3, Cu_8 and Cu_{13}.

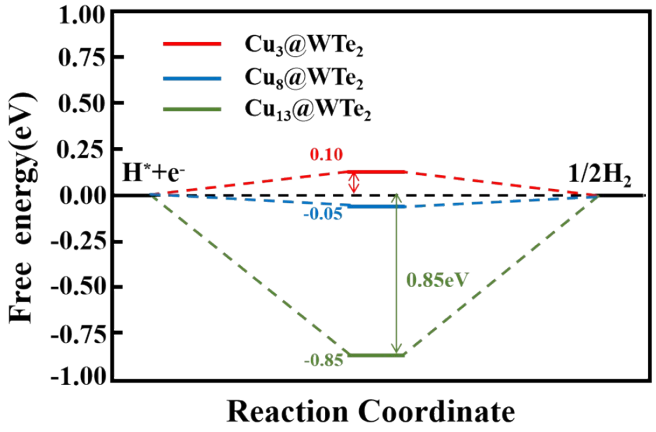

Fig. S14. The free energy changes for hydrogen evolution reaction (HER) on Cu_3@WTe_2, Cu_8@WTe_2, and Cu_{13}@WTe_2.

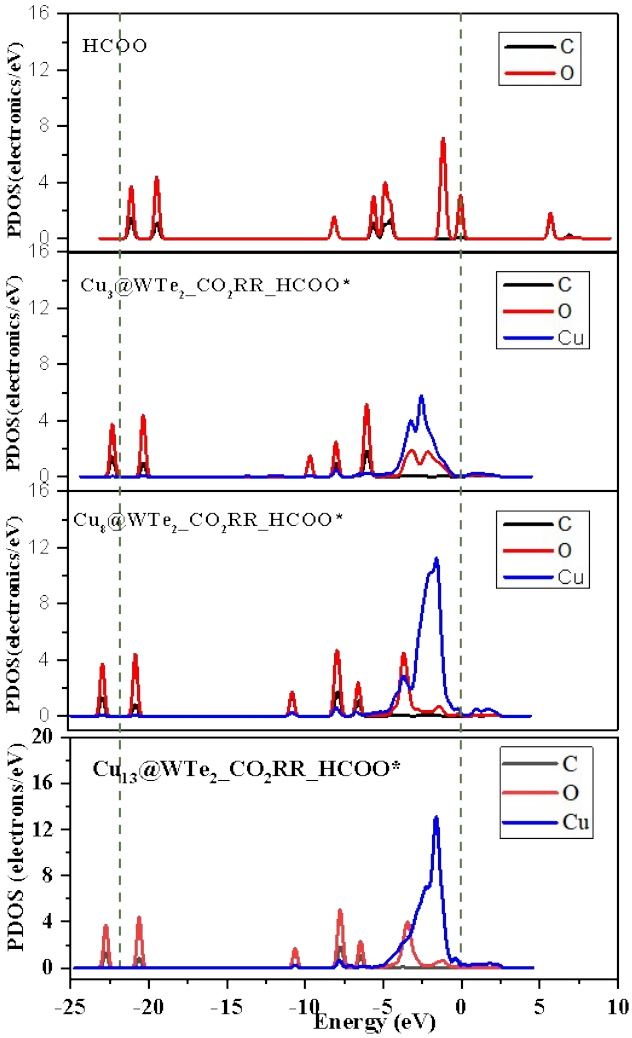

Fig. S15. (a) DOS of isolated HCOO intermediate and DOS of $Cu_3@WTe_2$(b), $Cu_8@WTe_2$ (c), $Cu_{13}@WTe_2$ after adsorption.

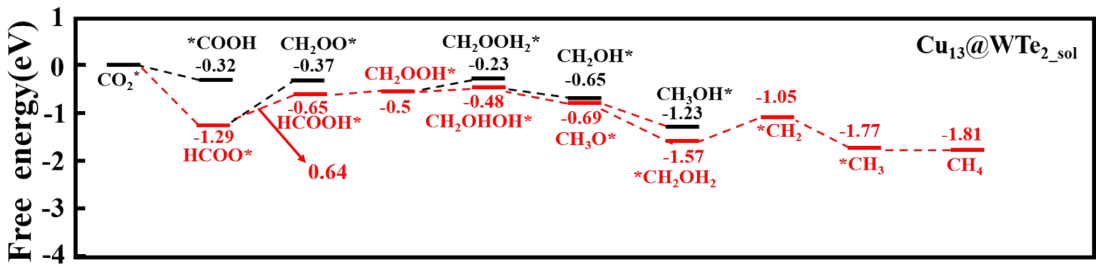

Fig. S16. Free energy diagram for the electrochemical CO_2RR with implicit solvation model on $Cu_{13}@WTe_2$

Table S1.

The calculated adsorption energies (E_{ads}) for Cu_n* on WTe_2 (n=3, 8, 13), the corresponding Cu-Cu bond lengths (L_{Cu-Cu}), and Cu-Te bond lengths (L_{Cu-Te}) of Cu_n@WTe_2 (n=3, 8, 13), the value of net electron transferred from Cu_n to WTe_2 (Δ q are calculated based on the Bader charges).

Adsorption configurations	**E_{ads} (eV)**	**L_{Cu-Cu} (Å)**	**L_{Cu-Te} (Å)**	**Δ q**
Cu_3@WTe_2	-3.92	2.48, 2.51, 2.68	2.66, 2.55, 2.63,	0.28
Cu_8@WTe_2	-4.72	2.43, 2.50, 2.42, 2.47	2.30, 2.57, 2.50, 2.67, 2.43, 2.80	0.32
Cu_{13}@WTe_2	-6.55	2.77, 2.50, 2.72, 2.68, 2.67	2.46, 2.52, 2.53, 2.58, 2.83	0.18

Table S2.

The calculated U_L ($|U_L|$), HCOO*/*COOH intermediate adsorption ($\Delta G_{HCOO*/*COOH}$) and final product of CO_2RR, and the H* intermediate adsorption(ΔG_{H*}) of HER with Cu_n@WTe_2(n=3,8,13) catalysts.

	CO_2RR			**HER**	
Configurations	**$\|U_L\|$**	**$\Delta G_{HCOO*/*COOH}$**	**Product**	**$\|U_L\|$**	**ΔG_{H*}**
Cu_3	0.64	-0.15	CH_4	0.51	-0.51
Cu_8	0.85	0.15	CH_4	0.73	0.73
Cu_{13}	0.89	-0.91	CH_4	0.14	-0.14
Cu_3@WTe_2	0.38	-0.27	CH_3OH	0.10	0.10
Cu_8@WTe_2	0.86	-1.04	CH_4	0.05	-0.05
Cu_{13}@WTe_2	0.55	-1.11	CH_4	0.85	-0.85

Table S3.

G (T) (T = 298.15K) value for CO_2RR process of CO_2* on Cu_3@WTe_2, Cu_8@WTe_2 and Cu_{13}@WTe_2.

Cu_3@WTe_2	G (T)	Cu_8@WTe_2	G (T)	Cu_{13}@WTe_2	G (T)
*CO_2	0.186231	*CO_2	0.185181	*CO_2	0.172623
HCOO*	0.414966	HCOO*	0.515557	HCOO*	0.512806
HCOOH*	0.777782	HCOOH*	0.762916	*OCHOH	0.75015
CH_2OOH*	1.093604	CH_2OOH*	1.078101	CH_2OOH*	1.083135
*$OHCH_2OH$	1.368316	CH_2O*+*OH_2	1.185102	CH_2O*+H_2O	0.616457
*CH_2OHOH_2	1.504707	CH_3O*	0.964499	CH_2OH*	0.980169
*CH_2OH	0.934407	CH_3OH*	1.267157	*CH_2+*OH_2	1.139901
*CH_3OH	1.228950	CH_4+*OH	0.229843	*CH_2	0.600369
		OH_2*	0.532801	*CH_3	0.82498
				CH_4	1.065491